with less than 180-mW dc power dissipation, and has a 10-MHz–2.0-GHz bandwidth with 16-dB gain. It has been concluded that the new circuit construction is effective for low-noise, low power-dissipation GaAs monolithic amplifiers. This amplifier is capable for use in mobile radio systems.

ACKNOWLEDGMENT

The authors wish to thank the members of the processing group for the fabrication, and also Dr. M. Ohmori for his constant encouragement.

REFERENCES

[1] K. Honjo, T. Sugiura, T. Tsuji, and T. Ozawa, "Low-noise, low-power-dissipation GaAs monolithic broadband amplifiers," in *Proc. 1982 GaAs IC Symp.*, pp. 87–90.
[2] M. Nishiuma, S. Katsu, S. Nambu, M. Hagio, and G. Kano, "A 2.2 dB NF 30–1700 MHz feedback amplifier," in *ISSCC Dig. Tech. Papers*, Feb. 1983, pp. 194–195.
[3] J. Tajima, Y. Yamao, T. Sugeta, and M. Hirayama, "GaAs monolithic low-power amplifiers with *RC* parallel feedback," *IEEE Trans. Microwave Theory Tech.*, vol. MTT-32, pp. 542–544, May 1984.
[4] T. Takada, M. Togashi, and T. Hirota, "GaAs MESFET circuit simulation model," in *Papers Techn. Group*, *TGSSD83-124*, IECE Japan, pp. 9–16.
[5] T. Takada, K. Yokoyama, M. Ida, and T. Sudo, "A MESFET variable-capacitance model for GaAs integrated circuit simulation," *IEEE Trans. Microwave Theory Tech.*, vol. MTT-30, pp. 719–724, May 1982.
[6] K. Yamasaki, K. Asai, T. Mizutani, and K. Kurumada, "Self-align implantation for N+-layer technology (SAINT) for high-speed GaAs IC's," *Electron. Lett.*, vol. 18, no. 3, pp. 119–121, Feb. 1982.
[7] M. Hirayama, M. Ino, Y. Matsuoka, and M. Suzuki, "A GaAs 4kb SRAM with direct coupled FET logic," in *ISSCC Dig. Techn. Papers*, Feb. 1984, pp. 46–47.
[8] D. B. Estrich, "A monolithic wide-band GaAs IC amplifier," *IEEE J. Solid-State Circuits*, vol. SC-17, pp. 1166–1173, Dec. 1982.
[9] J. A. Archer, H. P. Weidlich, E Pettenpaul, F. A. Petz, and J. Huber, "A GaAs monolithic low-noise broad-band amplifier," *IEEE J. Solid-State Circuits*, vol. SC-16, pp 648–652, Dec. 1981.
[10] M. Nishiuma, S. Nambu, M. Hagio, and G. Kano, "A GaAs monolithic low-noise wideband amplifier," presented at the 1981 Int. Symp. GaAs Related Compounds, 1981.
[11] W. C. Peterson, A. K. Gupta, and D. R. Decker, "A monolithic GaAs dc to 2 GHz feedback amplifier," in *IEEE 1982 Microwave Millimeter-wave Monolithic Circuits Symp. Dig. Tech. Papers*, June 18, 1982, pp. 20–22.

Polygonal Coaxial Line with Round Center Conductor

WEIGAN LIN

Abstract—**The complex potential function $W = A(\ln z + C_N z^N)$ generates a zero-potential line approximating a regular polygon of N sides very closely, except in the nearly field-free region. By means of this function we work out the characteristic impedance, the power-carrying capacity, and the attenuation constant of the polygonal line of N sides with a round inner coaxial conductor in a closed form of elementary functions with good accuracy compared to more complex solutions.**

Results for $N = 3$ are believed to be nearly as good as those available in the literature.

I. INTRODUCTION

Considerable work has been done on transmission lines in which the two conductors are not members of the same orthogonal cylindrical coordinate system. These are difficult electrostatic problems, one of which is the well-known charged sphere in a cylinder [1]. Riblet solved the characteristic impedance of a TEM coaxial line with a round inner and square outer conductor (shown in Fig. 1) and also of the related transmission line of a square inner and round outer conductor by means of a well-known transformation, work that first appeared in 1935 [2]. Subsequent work appeared in 1982 on this same problem [3], [7]. The purpose of this paper is to investigate the characteristics of the coaxial line with a round inner conductor of radius a and a polygonal outer conductor of N sides with an inscribed circle of radius b, as shown in Fig. 2. In comparison with the existing data, all our results are in closed forms, in elementary functions, and have accuracy nearly as good as data available in the literature, but the simplicity in the Z_0 formula surpasses all of them except for $N = 4$. The forms of our results allow us to calculate the power-carrying capacity and the attenuation constant of the line.

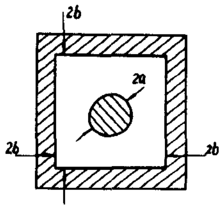

Fig. 1. TEM coaxial line with round inner and square outer conductor.

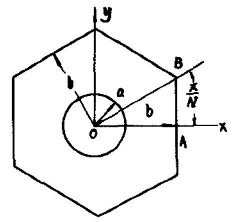

Fig. 2. TEM coaxial line with polygonal outer conductor of N sides and round inner conductor.

II. THE METHOD

We generalize Schelkunoff's work on the TEM transmission line with a round inner conductor and square outer conductor [4] by the following complex potential function:

$$W = U + jV = A\left[\ln\frac{z}{R} + C_N\left(\frac{z}{R}\right)^N\right] \tag{1a}$$

with

$$U = A\left[\ln\frac{\rho}{R} + C_N\left(\frac{\rho}{R}\right)^N \cos N\varphi\right] \tag{1b}$$

$$V = A\left[\varphi + C_N\left(\frac{\rho}{R}\right)^N \sin N\varphi\right] \tag{1c}$$

where (ρ, φ) are the polar coordinates, and A, R, and C_N are constants to be determined to fit the boundary conditions of the coaxial line of Fig. 2. If U and V are, respectively, the potential and the flux function, it follows that the charge per unit length Q of this coaxial line is

$$Q = \epsilon[V] = 2\pi\epsilon A. \tag{2}$$

Now C_N is nonzero, so the zero-potential line is determined by the following equation from (1b):

$$-C_N \cos N\varphi = \left(\frac{\rho}{R}\right)^{-N} \ln\frac{\rho}{R}. \tag{3}$$

Manuscript received January 25, 1984; revised January 14, 1985.
The author is with Chengdu Institute of Radio Engineering, Chengdu, Sichuan, 610054, People's Republic of China.

0018-9480/85/0600-0545$01.00 ©1985 IEEE

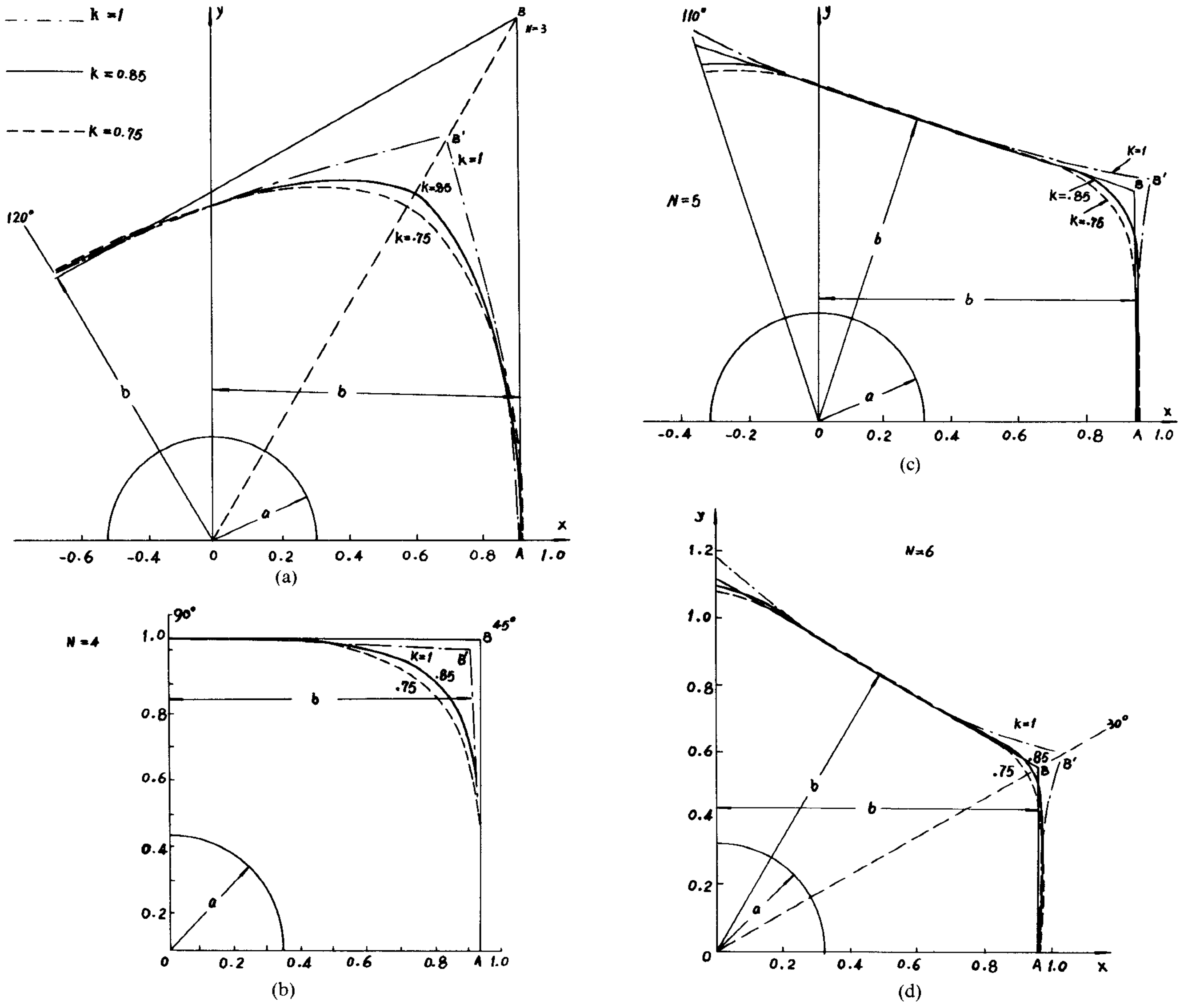

Fig. 3. The zero-potential lines for the polygonal coaxial lines, $K=1$, 0.85, and 0.75. (a) $N=3$, (b) $N=4$, (c) $N=5$, and (d) $N=6$.

We now write the right-hand side of (3) as $f(\rho)$; then

$$f(\rho)=\left(\frac{\rho}{R}\right)^{-N}\ln\frac{\rho}{R} \tag{4}$$

and $f'(\rho)=0$ gives $(\rho/R)^{-N-1}(1-N\ln\rho/R)=0$, or

$$\frac{\rho}{R}=e^{1/N} \tag{4a}$$

and it follows from (4) that $f(\rho)$ takes a maximum value

$$f(\rho)|_{\max}=\frac{1}{Ne}. \tag{4b}$$

Hence, (3) holds for $\cos N\varphi=-1$ or $\varphi=\pi/N$ only if $C_N\leqslant 1/Ne$, so we can introduce $k\leqslant 1$ to write

$$C_N=\frac{k}{Ne},\qquad k\leqslant 1 \tag{4c}$$

and the zero-potential curve or the contour of the ground outer conductor of the coaxial line, whose potential distribution is represented by (1b), is given by the following equation for arbitrary $k\leqslant 1$ by combining (3) and (4c):

$$\left(\frac{\rho}{R}\right)^{-N}\ln\left(\frac{\rho}{R}\right)^{-N}=kN\frac{1}{Ne}\cos N\varphi=\frac{k}{e}\cos N\varphi,\qquad k\leqslant 1. \tag{5}$$

We can then tabulate $X=(\rho/R)^{-N}$ versus $\Phi=N\varphi$ from (5) for various values of k, and from X and Φ we can plot the zero-potential curves for fixed N. We have drawn these for $k=1$, 0.85, and 0.75, for $N=3$, 4, 5, and 6 in Fig. 3.

From (5), we see immediately that when $\varphi=0$, ρ takes a minimum value $\rho_{\min}$, which can be found from (5) to satisfy the following relation:

$$\left(\frac{\rho_{\min}}{R}\right)^{-N}\ln\left(\frac{\rho_{\min}}{R}\right)^{-N}=\frac{k}{e},\qquad \varphi=0 \tag{6a}$$

respectively; for $k=1$, 0.85, and 0.75, we obtain from (6a)

$$\left(\frac{\rho_{\min}}{R}\right)^{-N}=1.32110,1.27737,1.24753 \tag{6b}$$

and when $N\varphi=\pi$ or $\varphi=\pi/N$, ρ/R takes the maximum value $\rho_{\max}/R$, and (5) goes into

$$\left(\frac{\rho_{\max}}{R}\right)^{-N}\ln\left(\frac{\rho_{\max}}{R}\right)^{-N}=-\frac{k}{e},\qquad \varphi=\pi/N \tag{7a}$$

to obtain, respectively, for $k=1,0.85,0.75$

$$\left(\frac{\rho_{\max}}{R}\right)^{-N}=0.3678794,0.587033,0.657173. \tag{7b}$$

TABLE I
MAXIMUM ρ/R AND MINIMUM ρ/R

k	$\rho_{max}/R, \varphi=\pi/N$				$\rho_{min}/R, \varphi=0$			
	$N=3$	$N=4$	$N=5$	$N=6$	$N=3$	$N=4$	$N=5$	$N=6$
$k=1$	1.39560	1.28402	1.221340	1.18135	0.911356	0.932752	0.945830	0.954650
$k=0.85$	1.19430	1.14244	1.11242	1.09284	0.921641	0.940635	0.952219	0.960021
$k=0.75$	1.15020	1.11065	1.08759	1.07247	0.928930	0.946210	0.956730	0.963810

We notice that, for $k=1$, we have already had, from (4a)

$$\frac{\rho_{max}}{R}=e^{1/N} \tag{7c}$$

which is the same as the first member of (7b).

Here, we tabulate only the values of ρ_{max}/R and ρ_{min}/R of the zero-potential line for $k=1$, 0.85, and 0.75 for the cases of triangular, rectangular, pentagonal, and hexagonal coaxial lines with round inner conductors, i.e., for $N=3$, 4, 5, and 6, in Table I.

Examining the zero-potential lines in Fig. 3(a)–(d) for $N=3$–6 plotted to scale, we may approximate the ground outer polygonal conductor of Fig. 2 by the zero-potential line (5) with $k=1$ as the best choice; then

$$\rho_{min}=b \text{ and } \rho_{max}=e^{1/N}R \tag{8}$$

by (4a). The inner conductor at a potential $(-U_1)$, of Fig. 3 is to be approached by the following locus:

$$-U_1=A\left[\ln\frac{\rho}{R}+\frac{1}{Ne}\left(\frac{\rho}{R}\right)^N\cos N\varphi\right] \tag{9a}$$

and if ρ/R is not too large, we have nearly

$$U_1=A\ln\frac{R}{\rho} \tag{9b}$$

a circle when $U_1=$ constant and which can be made to coincide with the round inner conductor by putting $\rho=a$; then

$$A=U_1/\ln\frac{R}{a}. \tag{9c}$$

We now demonstrate that (1b) is indeed a closed curve approaching a circle. Using (9c), we write the potential function (1b) as

$$U=\frac{U_1}{\ln\frac{R}{a}}\left[\ln\frac{\rho}{R}+\frac{1}{Ne}\left(\frac{\rho}{R}\right)^N\cos N\varphi\right].$$

When $U=-U_1$, this equation becomes

$$\ln\frac{\rho}{R}+\frac{1}{Ne}\left(\frac{\rho}{R}\right)^N\cos N\varphi=-\ln\frac{R}{a}.$$

Collecting terms, we have an equipotential of the form

$$\ln\frac{\rho}{a}+\frac{1}{Ne}\left(\frac{a}{R}\right)^N\left(\frac{\rho}{a}\right)^N\cos N\varphi=0. \tag{10}$$

Now it is seen from (10a) that

$$R>b>a$$

so when $N\geqslant 3$, $(a/R)<a/b$ and a/b is small, the equipotential (10) becomes nearly

$$\ln\rho/a=0, \qquad \rho=a$$

a circle to approximate the inner circular conductor.

Thus, we may take the zero-potential curve AB' for $C_N=1/Ne$, i.e., $k=1$ in Fig. 3(a)–(d) to replace the half-side AB of the polygonal outer conductor, and we may also take the concentric circle $\rho=a$ to be the inner equipotential line of $U=-U_1$ in order to study the operating characteristics of the TEM line of the polygonal outer conductor and round inner conductor of Fig. 2 under study. Before we proceed, we need still to fix the constant R in (1). From (6b), for $k=1$, we have from (8)

$$R=(1.32110)^{1/N}b. \tag{10a}$$

Also fixed is ρ_{max}

$$\rho_{max}=(1.32110e)^{1/N}b. \tag{10b}$$

Already we have made

$$\rho_{min}=b. \tag{10c}$$

III. FIELD DISTRIBUTION

From the zero-potential lines in Fig. 3 and from Table I, we can see that, along the line $\varphi=\pi/N$, we can change ρ_{max} by a large amount with only a slight change in ρ_{min} in the same zero-potential line to maintain the potential zero. We thus see that in the neighborhood of each interior angle there is a field-free region. That is why we are at ease to replace the half-side of AB by the curved zero-potential line of (5) for $k=1$.

From (1a), we have for the magnitude of the electric field E inside the transmission line as

$$|E|=\left|\frac{dw}{dz}\right|=A\left|\frac{1}{z}\left\{1+NC_N\left(\frac{z}{R}\right)^N\right\}\right|.$$

Recalling $z=\rho e^{j\varphi}$, we have then

$$|E|^2=\frac{A^2}{\rho^2}\left\{1+\left(NC_N\frac{\rho^N}{R^N}\right)^2+2NC_N\frac{\rho^N}{R^N}\cos N\varphi\right\}. \tag{11a}$$

Along the zero potential, (5) holds for $k=1$; (11a) goes into

$$|E|^2=\frac{A^2}{\rho^2}\left\{1+\frac{1}{e^2}\left(\frac{\rho}{R}\right)^{2N}-\ln\left(\frac{\rho}{R}\right)^{2N}\right\} \tag{11b}$$

so that by (6b) and (7c), (11b) gives

$$|E|=0 \text{ at } \varphi=\pi/N, \qquad \rho=\rho_{max} \tag{12a}$$

and at point A of Fig. 2, (11b) gives

$$|E|_A^2=\frac{A^2}{b^2}\left\{1+(1.3211e)^{-2}+2\ln 1.3211\right\}=\frac{A^2}{b^2}(1.2785)^2$$
$$=\frac{A^2}{(0.7822b)^2} \tag{12b}$$

independent of the number of sides N. Around the round inner conductor, the electric field is given by

$$|E|=\frac{A}{a}. \tag{12c}$$

Therefore, in the interior of the TEM line of Fig. 3, when AB is replaced by AB', the electric field at point A is 1.2785 times the field that would exist if the outer conductor were a round

TABLE II
THE CHARACTERISTIC IMPEDANCE OF THE POLYGONAL LINE WITH CYLINDRICAL CENTER CONDUCTOR

	N = 3			N = 4			
					Gunston [6] based on		
a/b	Present work (Ohms)	Seshagiri [6] § 5.62 (Ohms)	Seshadri and Rajaian [7] (Ohms)	Present work (Ohms)	Lin & Chung [6] § 4.2(d) (Ohms)	Seshagiri [6] § 5.62 (Ohms)	Seshadri and Rajaiah [7] (Ohms)
0.05	185.16	184.32	187.317	183.77	184.14	183.28	184.417
0.1	144.36	142.58	145.700	142.21	142.59	141.58	142.799
0.2	102.05	100.86	104.082	100.66	101.03	99.87	101.182
0.3	77.74	76.55	79.735	76.35	76.72	75.50	76.837
0.4	60.49	59.42	62.454	59.10	59.48	58.27	59.563
0.5	47.12	46.24	49.029	45.73	46.10	44.95	46.161
0.6	36.19	35.55	38.006	34.80	35.16	34.11	35.197
0.7	26.94	26.52	26.568	25.55	25.90	24.97	25.886
0.8	18.94	18.59	20.135	17.55	17.81	16.99	17.706
0.9	11.88	11.17	12.061	10.49	10.41	9.72	10.146

	N = 5		N = 6	
a/b	Present work (Ohms)	Seshagiri [6] § 5.62 (Ohms)	Present work (Ohms)	Seshagiri [6] § 5.62 (Ohms)
0.05	182.94	182.58	182.38	181.64
0.1	141.38	140.92	140.82	140.01
0.2	99.83	99.26	99.27	98.38
0.3	75.52	74.91	74.96	74.04
0.4	58.27	57.65	57.71	56.79
0.5	44.89	44.30	44.34	43.43
0.6	33.97	33.42	33.41	32.58
0.7	24.72	24.24	24.16	23.34
0.8	16.72	16.26	16.16	15.37
0.9	9.66	9.06	9.10	8.25

conductor of radius b by (12b), independent of N. By comparing (12b) and (12c), it follows that the maximum field will occur at point A of Fig. 2 given by (12b) when

$$0.7822 < \frac{a}{b} < 1 \tag{13a}$$

and the maximum field will occur at the surface of the round inner conductor given by (12c) if

$$\frac{a}{b} < 0.7822. \tag{13b}$$

The constant is given by (9b), or

$$A = U_1 / \ln \frac{R}{a}. \tag{14}$$

IV. CHARACTERISTIC IMPEDANCE

The characteristic impedance of the polygonal line with a round inner conductor is given by

$$Z_0 = \sqrt{\frac{\mu}{\epsilon}}\,\frac{1}{C/\epsilon}$$

where C is the capacitance per unit length of the line given by

$$C = \frac{Q}{U_1}$$

where Q is given by (2) and U_1 by (9b), so

$$Z_0 = \frac{1}{2\pi}\sqrt{\frac{\mu}{\epsilon}}\ln\frac{R}{\rho_1} = \frac{1}{2\pi}\sqrt{\frac{\mu}{\epsilon}}\left\{\ln\frac{b}{a} + \frac{1}{N}\ln 1.32110\right\}$$

$$= 59.952\left(\ln\frac{b}{a} + \frac{0.27847}{N}\right). \tag{15a}$$

For $N = 4$, we have (we use here 59.952 according to [6], it would have been 59.9585 according to Cohn [5])

$$Z_0 = 59.952\left(\ln\frac{b}{a} + 0.06962\right) \tag{15b}$$

which is slightly different from that given by Schelkunoff [4]. Schelkunoff's work is found to be in agreement with the result given by Frankel [6], being virtually exact for

$$\frac{a}{b} < 0.65 (Z_0 > 30\Omega)$$

and giving an error within 1.5 percent for

$$\frac{a}{b} < 0.80$$

according to Cohn [5]. One referee points out that the constant in (15a) in the limit $a \to 0$ is $\ln 2/K(0.707) = 0.07576$ according to Oberbettiger and Magnus (Springer-Verlag, Berlin, 1949).

We calculate Z_0 for $N = 3$, 4, 5, and 6 to be compared with the work of various authors (see Table II). In Fig. 3(a) and (b), $N = 3$ and 4, and B' is nearer to the origin than B; thus, the impedances given by (15a) are lower bounds to the true values, so the higher the better. Values for $N = 3$ are between those given by [6] and [7] as shown in Table I, $N = 3$, and thus are better than those given by [6]. When $N = 4$, values given by (15b) likewise are better than those from Seshagiri [6]. Since Gunston claims that by taking the geometric mean of the bounds given by Lin and Chung, the values of [6] § 4.2d are the most accurate results then available, and values obtained from (15b) are very close to those of [6] § 4.2d (reproduced in Table II), and so are of very good accuracy and in neat closed form!

In Fig. 3(c) and (d), $N = 5$ and 6, and B' is farther from the origin than B, so Z_0 given by (15a) are upper bounds to the true values; thus, they are very slightly greater than those from [6], and are accurate enough for practical purposes, Z_0 being in closed form (15a).

V. Power-Carrying Capacity

The power transmitted down the transmission line is given by

$$P = \frac{U_1^2}{Z_0} = \frac{A^2 \ln \frac{R}{a}}{\frac{1}{2\pi}\sqrt{\frac{\mu}{\epsilon}}}. \tag{16}$$

The power-carrying capacity of the transmission line is determined by the maximum electric field in the interior of the transmission line, and is given by

$$P_{\max} = 10.21 \times 10^{-3} (E_{\max} b)^2 \left\{ \ln \frac{b}{a} + \frac{0.27847}{N} \right\}, \mathrm{W} \tag{17a}$$

if

$$0.7822 < \frac{a}{b} < 1$$

by (12b) and (15a), and $E_{\max}$ occurs at A on the outer conductor, and

$$P_{\max} = 16.68 \times 10^{-3} (a E_{\max})^2 \left\{ \ln \frac{b}{a} + \frac{0.27847}{N} \right\} \tag{17b}$$

if

$$\frac{a}{b} < 0.7822$$

and $E_{\max}$ occurs on the inner round conductor independent of φ. In both (16a) and (16b), $E_{\max}$ is the maximum allowable voltage gradient; a value of 30 000 V/cm is applicable for air-filled lines under standard sea-level conditions of temperature, pressure, and humidity.

In place of (14), we can determine the constant A by (16)

$$A = 7.743 \sqrt{\frac{P}{\ln \frac{b}{a} + \frac{0.27847}{N}}}. \tag{18}$$

VI. Attenuation Constant

The attenuation constant α of a transmission line supporting a TEM mode can be expressed in terms of line integrals of the electric field normal to the inner boundary S_1 and outer conductor S_2

$$\alpha = \frac{1}{2} \frac{1}{\sigma\delta} \frac{\epsilon}{\mu} \frac{\oint_{S_1+S_2} |E|^2 \, dl}{P}, \text{ neper/m} \tag{19}$$

where σ is the conductivity of the inner and the outer conductors, δ is the skin depth, P is given by (16), S_1 is the circle of radius a, and S_2 may be taken as $2N$ times AB of Fig. 2 and Fig. 3(a)–(d) to approach the true zero-potential AB', so that, by putting in (11b), we have

$$\oint_{S_2} |E|^2 \, de = 2N \int_0^{b \tan \pi/N} A^2 \frac{dy}{(b^2+y^2)} \cdot \left\{ 1 + 2N \ln R + \frac{1}{e^2 R^{2N}} (b^2+y^2)^N - N \ln (b^2+y^2) \right\}$$

$$= \frac{2NA^2}{b} \left\{ \frac{\pi}{N} \left[1 + \ln \left(\frac{R}{b} \right)^{2N} \right] + \frac{1}{(1.3211)^2} \int_0^{\pi/N} (\sec\theta)^{2N} \, d\theta - 2N \int_0^{\pi/N} \ln \sec 0 \, d\theta \right\}$$

$$= \frac{2NA^2}{b} \left\{ \frac{\pi}{N}(1.55694) + 0.077543 \int_0^{\pi/N} (\sec\theta)^{2N} \, d\theta - \int_0^{\pi/N} \ln (\sec\theta)^{2N} \, d\theta \right\}. \tag{20a}$$

From (12c), we find that

$$\oint_{S_1} |E|^2 \, dl = 2\pi A^2 / a. \tag{20b}$$

Therefore, (19) goes into

$$\alpha = \frac{1}{2\sigma\delta} \sqrt{\frac{\epsilon}{\mu}} \frac{\left(\frac{1}{a} + \frac{f_N}{b} \right)}{\ln \frac{b}{a} + \frac{0.27847}{N}}$$

$$= \frac{1.3273 \times 10^{-3}}{b} \frac{1}{\sigma\delta} \frac{\frac{b}{a} + f_N}{\ln \frac{b}{a} + \frac{0.27847}{N}}, \text{ neper/m} \tag{20b}$$

where

$$f_N = 1.45694 + 0.024683 N \int_0^{\pi/N} (\sec\theta)^{2N} \, d\theta - \frac{N}{\pi} \int_0^{\pi/N} \ln (\sec\theta)^{2N} \, d\theta$$

$f_N = 0.864738$ for $N = 3$

$f_N = 0.744186$ for $N = 4$

$f_N = 0.667189$ for $N = 5$

$f_N = 0.662077$ for $N = 6$.

From (20), it follows that, for fixed b, α has its minimum value at a value of b/a, which satisfies the following equation:

$$\ln \frac{b}{a} - f_N \frac{a}{b} - \left(1 - \frac{0.27847}{N} \right) = 0. \tag{21}$$

For instance, $N = 4$, $(b/a) = 3.2$. This should be contrasted with the value of $(b/a) = 3.6$ for a regular coaxial line. Equation (20) goes into the attenuation constant for a regular coaxial line if $N \to \infty$ and $f_N \to 1$.

VII. Conclusion

Generalizing Schelkunoff's idea on the perturbation of boundaries to obtain the potential function of (1b), we find that the zero-potential boundary has the same symmetry as the regular polygon of N sides and approximates the latter very closely. The fact that this approximation is better on the portion of the side of the polygonal outer conductor AB of Fig. 3(a)–(d), when this line segment lies closer to the point of the minimum radius vector $\rho_{\min}$, where the electric field is strong, and that this approximation is poor only in the nearly field-free region, such as in the interior angle near the vertex B of Fig. 3(a)–(d), convinces us of the feasibility of the application of the complex potential function (1a) to the transmission-line problem of Fig. 2 and the reasonable accuracy of the results on impedance, power capacity, and attenuation of this line. It is claimed in [7] that the results found there for the characteristic impedance were superior to those available then in the literature. Results presented in this paper (Table II and Fig. 3(a)) support this claim [7]. All the expressions for the characteristic impedances presented in this paper are believed to be accurate enough for practical purposes, are all in closed form, and are easily manipulated. Wheeler [8] gives a more accurate and useful analysis, but his results are more complicated. Other good work (such as [9]) exists, but their results are also more complicated. The attenuation constant formula given here is only approximately correct, and may be of value for a quick estimation, and it happens often that experimental values of the attenuation constant show a marked deviation from theoretical values!

References

[1] W. R. Smythe, "Charged sphere in cylinder," *J. Appl. Phys.*, vol. 31, no.3, pp. 532–553, Mar. 1960.

[2] H. J. Riblet, "An accurate determination of the characteristic impedance of the coaxial system consisting of a square concentric with a circle," *IEEE Trans. Microwave Theory Tech.*, vol. MTT-23, pp. 714–715, Aug. 1975.

[3] W. Lin, "A critical study of the coaxial transmission line utilizing conductors of both circular and square cross section," *IEEE Trans. Microwave Theory Tech.*, vol. MTT-30, pp. 1981–1988, Nov. 1982.

[4] S. A. Schelkunoff, *Applied Mathematics for Engineers and Scientists* New York: Van Nostrand, 1948, p. 298.

[5] S. B. Cohn, "Beating a problem to death," *Microwave J*, vol. 12, no. 11, pp. 22–23 Nov. 1969; p. 20, Sept. 1968.

[6] M. A. R. Gunston, *Microwave Transmission Line Impedance Data.* New York: Van Nostrand Reinhold, 1972, § 4 2 and Table 5 2.

[7] T. K. Sheshadri and K. Rajaiah, "Accurate estimation of characteristic impedance of coaxial transmission-line problems by the eigenfunction approach," *Proc. IEEE*, vol. 70, pp. 82–83, Jan. 1982.

[8] H. A. Wheeler, "Transmission-line properties of a round wire in polygon shield," *IEEE Trans. Microwave Theory Tech.*, vol. MTT-27, pp 717–721, Aug. 1979.

[9] P. A. A. Laura and L. E. Luisoni, "Approximate determination of the characteristic impedance of the coaxial system concentric with a circle," *IEEE Trans. Microwave Theory Tech.*, vol. MTT-25, pp. 160–161, Feb. 1977.

Impedance of an Elliptic Conductor Arbitrarily Located Between Ground Planes Filled with Two Dielectric Media

K. V. SESHAGIRI RAO, MEMBER, IEEE, AND B. N. DAS

Abstract —**This paper presents a method of determining the characteristic impedance of an ellipse arbitrarily located between parallel conducting planes when the region between the planes is filled with two different dielectric media. The same generalized formulation is then extended to the case when one of the ground planes is moved to infinity. The impedance data for various locations of the dielectric interface with respect to the conductor of elliptic and circular cross sections are presented. The results of some of the special cases are compared with those available in the literature [2].**

I. Introduction

The method of analysis of transmission-line properties of parallel strips separated by a dielectric was carried out by Wheeler in 1965 [1]. He has also analyzed the properties of a round wire in a cylindrical shield of polygonal cross section [2]. Later studies were made on an offset stripline and microstripline using planar strip when the line is filled with two dielectric media [3]. The analysis of transmission line for the case when the center conductor assumes the form of an ellipse arbitrarily located between ground planes or placed above a single ground plane has been carried out by the authors [4].

In the present work, the generalized conformal transformation obtained for the conductor with an elliptic boundary is used for the estimation of impedance data when the region between the ground planes of the line is filled with two different dielectric media. This analysis is based on the quasi-TEM-mode approximation and, hence, is valid at the lower frequency ranges only. The conformal transformation transforms one half of the structure into a parallel-plate configuration in which the top and bottom plates correspond, respectively, to the conductor with the curved boundary and the ground planes. In this transformed parallel-plate configuration, the dielectric interface appears in the form of a curved contour. The characteristic impedance of this composite parallel-plate structure is calculated by considering the series parallel combinations of small incremental capacitances [1]. The expressions for these capacitances appear in the form of integrals which are numerically evaluated using the adaptive quadrature method [5].

The formulation is used for the computation of characteristic impedances for the cases of a center conductor 1) placed exactly above the dielectric interface, 2) placed such that one of the principal axes is coplanar with the dielectric interface, and 3) fully embedded in the dielectric.

II. Formulation for the Case of an Ellipse Embedded in Mixed Dielectrics Between Ground Planes

Consider the configuration shown in Fig. 1(a). The method of transforming the half *FABCDEF* into a parallel-plate configuration as shown in Fig. 1(b) has already been developed by the authors [4]. The transformation establishes the relation between the points in the W-plane (Fig. 1(b)) with those of the corresponding points in the Z-plane (Fig. 1(a)). The corresponding loci in the two planes (Z and W planes) can also be determined. The equations for the lines parallel and perpendicular to the two ground planes in the W-plane are given by [6]

$$u' = -\frac{1}{K(m)}\left[F(\beta|m) + F\left(\sin^{-1}\sqrt{\frac{n}{m}}\,\middle|\,m\right)\right] \qquad (1)$$

$$\frac{v'}{V_0} = 1 - \frac{F(\gamma|m_1)}{K'(m)} \qquad (2)$$

where m, n are constants, $0 < n < m < 1$, and where F and K correspond, respectively, to incomplete and complete elliptic integrals of the first kind with given argument and modulus. β and γ are real arguments of the elliptic integrals. The elliptic integral with complex argument Φ can be expressed as

$$F(\Phi|m) = F(\eta + i\xi|m) = F(\beta|m) \pm iF(\gamma|m_1)$$

$$t_r = \cosh\xi\sin\eta = \frac{\sin\beta\sqrt{1 - m_1\sin^2\gamma}}{\cos^2\gamma + m\sin^2\beta\sin^2\gamma}$$

$$t_i = \cosh\eta\sinh\xi = \frac{\cos\beta\cos\gamma\sin\gamma\sqrt{1 - m\sin^2\beta}}{\cos^2\gamma + m\sin^2\beta\sin^2\gamma}$$

$$t = t_r + it_i = \sin\Phi, \qquad m_1 = (1 - m).$$

U_0 and V_0 shown in Fig. 1(b) are given by

$$U_0 = 1 + \frac{F\left(\sin^{-1}\sqrt{n/m}\,|m\right)}{K(m)} \qquad (3)$$

$$V_0 = \frac{K'(m)}{K(m)}. \qquad (4)$$

Manuscript received January 23, 1984; revised January 25, 1985.

K. V. S. Rao is with the Centre for Research and Training in Radar and Communication, Indian Institute of Technology, Kharagpur 721302, India.

B N Das is with the Department of Electronics and Electrical Communication Engineering, Indian Institute of Technology, Kharagpur 721302, India.

0018-9480/85/0600-0550$01.00 ©1985 IEEE